Vibrational Sum Frequency Scattering from a Submicron Suspension

Sylvie Roke,[1,*] Wim G. Roeterdink,[1] Judith E. G. J. Wijnhoven,[2] Andrei V. Petukhov,[2] Aart W. Kleyn,[1,3] and Mischa Bonn[1]

[1]*Leiden Institute of Chemistry, P.O. Box 9502, 2300 RA Leiden, The Netherlands*
[2]*Debye Institute, Utrecht University, P.O. Box 80051, 3508 TB Utrecht, The Netherlands*
[3]*FOM-Institute Rijnhuizen, P.O. Box 1207, 3430 BE Nieuwegein, The Netherlands*

(Received 3 June 2003; published 19 December 2003)

A novel application of vibrational sum frequency generation (VSFG) is developed to study the molecular properties of the surface of submicron particles in suspension. The Rayleigh-Gans-Debye scattering theory is extended to extract the local molecular response from the macroscopic nonlinearly scattered spectral intensity. These results demonstrate the use of VSFG to investigate quantitatively the surface molecular properties of submicron particles, dispersed in solution. It provides information on the order and density of alkane chains and allows us to determine the elements of the local second-order surface susceptibility.

DOI: 10.1103/PhysRevLett.91.258302 PACS numbers: 82.70.Dd, 42.65.–k, 68.60.–p, 78.68.+m

Second-order nonlinear optical spectroscopies have become well-established and versatile tools to investigate planar interfaces, because of their sensitivity to broken inversion symmetry. Particularly vibrational sum frequency generation (VSFG) has emerged as an important technique in surface studies, owing to its molecular surface specificity [1–6]. It allows one to, e.g., determine the orientation and molecular order of molecules constituting biological membranes and Langmuir-Blodgett films [7–12]. Ideally, one would want to enjoy the advantages of VSFG to obtain information on nonplanar local surfaces of, e.g., liposomes and cells. Although the inherent macroscopic inversion symmetry in these media seems to exclude the application of VSFG to such systems, recent experimental [13,14] and theoretical [15] reports of second harmonic generation provide good prospects. In addition, reflection sum frequency experiments have been successfully performed on strongly corrugated surfaces comprised of micron-sized powdered crystalline particles [16], 15 nm gold nanoparticles deposited on water and silicon/air interfaces [17], and 200 nm latex beads at the air/liquid, and air/solid interface [18]. These observations suggest that it should, in principle, be possible to probe the usually weak vibrational modes of molecules on the surface of submicron particles in a dilute suspension.

In this Letter we demonstrate the use of VSFG to study the interface of submicron particles in suspension. As a model system we use a suspension of silica particles covered with alkane chains anchored by one end to the sphere. We obtain information on the molecular order and density of the molecules at the surface by analyzing both the vibrational response and the angle dependent scattered intensity, as a function of polarization of the incident and emitted fields. The Rayleigh-Gans-Debye scattering theory is further developed to extract local second-order nonlinear susceptibility elements from the macroscopic scattered spectral intensity. The results demonstrate the possibility of using VSFG to investigate the molecular properties of the nonplanar surface of submicron particles dispersed in a solution.

The VSFG experiments were performed using 10 μJ (120 fs) infrared (IR) pulses (repetition rate 1 kHz, FWHM bandwidth of $\sim$180 cm^{-1}) centered around 2900 cm^{-1} and 3.0 μJ, 800 nm visible (VIS) pulses with a 10 cm^{-1} bandwidth. A schematic representation of the experimental geometry can be found in Fig. 1 (left panel). The selectively polarized IR and VIS pulses were incident under a relative angle of 15° (β) and focused down to a $\sim$0.4 mm beamwaist. The scattered light was collimated with a lens, polarization selected and dispersed onto an intensified charge coupled device camera [19,20]. Typical recording times were $\sim$600 s. The

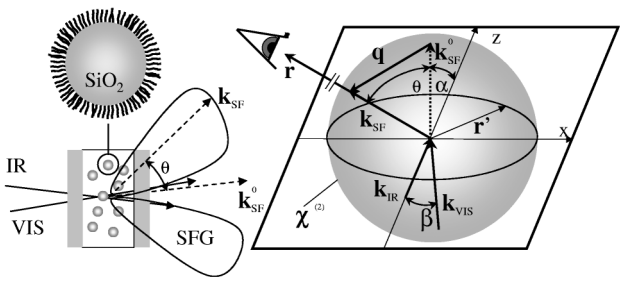

FIG. 1. Left panel: the experimental geometry, with a schematic illustration of one particle. Right panel: the scattering geometry. $\mathbf{k}_{IR}$ is the wave vector of the IR field, $\mathbf{k}_{VIS}$ is the wave vector of the VIS field, $\mathbf{k}_{SF} = k_{SF}\hat{\mathbf{n}}$ is the wave vector of the scattered sum frequency field, $\mathbf{k}_{SF}^{0} = \mathbf{k}_{IR} + \mathbf{k}_{VIS}$, $\mathbf{q}$ is the scattering wave vector, $\mathbf{r} = r\hat{\mathbf{n}}$ is the detector position, and $\mathbf{r}'$ is a point on the surface of the sphere. All $\mathbf{k}$ vectors and $\mathbf{r}$ lie in the horizontal x-z plane. The IR, VIS, and SFG fields are either polarized parallel (H) or perpendicular (V) to the scattering plane.

angular resolution was controlled by an aperture placed in front of the collimating lens and was typically 12°.

The samples consist of dry stearic alcohol ($C_{18}H_{37}OH$) coated [21] silica particles [22] dispersed in CCl_4 (99.9%, Baker Analyzed) with a colloid volume fraction of 4.4%. The sample cell consists of two CaF_2 plates separated by a 1 mm Teflon spacer. In this Letter we report on particles with a radius (R) of 342 nm ± 36 nm and a spherical shape factor of 0.98. The particle size distribution was determined from an analysis of transmission electron microscopy (TEM) images containing several hundred colloids (see Fig. 2). Particles with radii ranging from 69 up to 605 nm have been investigated, with results similar to those presented here. Before each measurement the samples were put in an ultrasonic bath for several minutes, to ensure the absence of aggregates.

Figure 2 shows four VSFG spectra recorded with different polarization combinations denoted in the graph, at a scattering angle (θ) of 22°. To ascertain that the signal originates from the colloids in suspension and not from those adsorbed to the sample window, we have measured the total SFG intensity as a function of sample position along the z axis (shown in the bottom right). The solid line is a calculation assuming a signal originating from the colloids in the suspension and the dashed line represents the case of a signal originating from colloids adsorbed to the walls. Clearly, the measured intensity originates from the particles in the suspension. That the signal does not originate from a macroscopic interface is further corroborated by the observation that no signal was present in the macroscopic phase matched direction (along $\mathbf{k}_{SF}^{0}$). The signal vanishes upon replacing the suspension with pure CCl_4. No signal was observed for any other polarization combination.

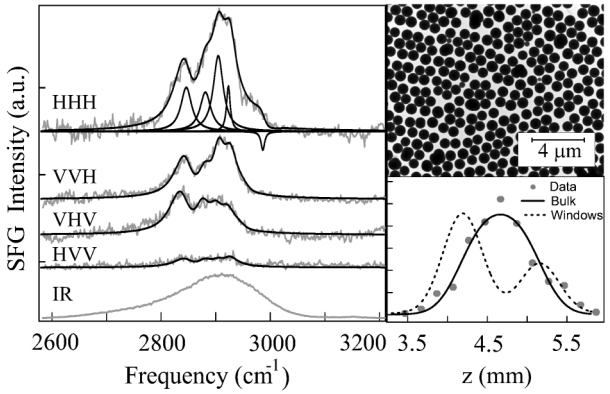

FIG. 2. Left panel: VSFG spectra (gray lines) and fits (black lines) obtained at different polarization conditions (the three letter codes next to the spectra indicate (H for horizontal, V for vertical) polarizations for SFG, VIS, and IR, respectively) at a scattering angle of 22°. The angular resolution was 12°. The intensities are corrected for polarization dependent detector sensitivity. The black lines are fits as described in the text. The solid lines in the upper trace (HHH) represent the squared IR amplitude functions used in the fitting procedure with the sign indicating the relative phase. The bottom trace depicts an SFG spectrum from a gold surface, which reflects the IR pulse bandwidth. Top right: TEM image of the colloids. Bottom right: integrated SFG intensity as a function of sample position. The solid (dashed) line represents the calculated signal originating from colloids in the suspension (adsorbed to the windows).

To obtain meaningful information from these spectra we describe the generated sum frequency field in terms of the local components of the second-order nonlinear surface susceptibility, $\boldsymbol{\chi}^{(2)}$, for each vibrational mode. As the colloid surfaces can be considered locally isotropic, there are four nonzero elements of $\boldsymbol{\chi}^{(2)}$(for each mode): $\chi^{(2)}_{\perp\perp\perp}$, $\chi^{(2)}_{\perp\parallel\parallel}$, $\chi^{(2)}_{\parallel\perp\parallel}$, and $\chi^{(2)}_{\parallel\parallel\perp}$ contributing to the second-order nonlinear polarization at the surface of the sphere, $\mathbf{P}^{(2)}_{SF}(\mathbf{r}')$ [$\perp$ ($\parallel$) refers to the direction perpendicular (parallel) to the local surface normal]. $\mathbf{P}^{(2)}_{SF}$ is a function of the local infrared $\mathbf{E}_{IR}$ and visible $\mathbf{E}_{VIS}$ fields: $\mathbf{P}^{(2)}_{SF}(\mathbf{r}') = \sum_n \boldsymbol{\chi}^{(2)}_n : \mathbf{E}_{IR}(\mathbf{r}')\mathbf{E}_{VIS}(\mathbf{r}')$, where n refers to the vibrational mode. For dilute suspensions the total scattered intensity is the incoherent sum of the intensities scattered by the individual colloids [23]. We can describe the scattering field outside one spherical particle as a function of the scattering angle (θ) by solving the wave equation (with the local second-order nonlinear polarization as the source term) using a Green's function method [24]:

$$\mathbf{E}_{SF}(\mathbf{r}) = \frac{1}{\epsilon}\nabla \times \nabla \times \int d\mathbf{r}' \frac{e^{i\mathbf{k}_{SF}\cdot|\mathbf{r}-\mathbf{r}'|}}{|\mathbf{r}-\mathbf{r}'|}\mathbf{P}^{(2)}_{SF}(\mathbf{r}') \quad (1)$$

in which $\mathbf{k}_{SF}$ is the scattering wave vector, ϵ is the dielectric constant of the solvent, $\mathbf{r} = r\hat{\mathbf{n}}$ is the position of the detector, and $\mathbf{r}'$ is the local coordinate at the surface of the sphere ($|\mathbf{r}'| = R$). Thus, the phase relation between light generated at different parts of the sphere is fully taken into account in the analysis. As detection occurs in the far field we can safely assume that $R \ll r$. Since the refractive indices of the solvent and the particle are almost identical ($n_{CCl_4} = 1.4579$ [25] and $n_{SiO_2} = 1.42$, as determined from linear optical measurements at 645 nm), we can use the Rayleigh-Gans-Debye (RGD) approximation [13,14], which treats the electric fields inside and outside the sphere as identical [24]. Inserting $\mathbf{P}^{(2)}_{SF}(\mathbf{r}')$ with $\mathbf{E}^{(2)}_i(\mathbf{r}') = E_i e^{i\mathbf{k}_i\cdot\mathbf{r}'}\mathbf{e}_i$. Equation (1) becomes

$$\mathbf{E}_{SF}(r) = -E_{IR}E_{VIS}k^2_{SF}\frac{e^{ik_{SF}r}}{\epsilon r}\hat{\mathbf{n}} \times \left\{\hat{\mathbf{n}} \times \int d\mathbf{r}' e^{i\mathbf{q}\cdot\mathbf{r}'}\left[\sum_\gamma\left(\sum_{\alpha,\beta}\chi^{(2)}_{\gamma\alpha\beta}(\mathbf{e}_\alpha\cdot\mathbf{e}_{IR}) \times (\mathbf{e}_\beta\cdot\mathbf{e}_{VIS})\mathbf{e}_\gamma\right)\right]\right\}. \quad (2)$$

In the above expression $\chi^{(2)}_{\gamma\alpha\beta}$ are the elements of the local second-order nonlinear surface susceptibility. $\mathbf{e}_{\alpha,\beta,\gamma}$ correspond to the unit vectors of the local (spherical) coordinate system, $\mathbf{e}_{IR,VIS}$ are the unit polarization vectors of the incoming beams, $\mathbf{k}_{SF} = k_{SF}\hat{\mathbf{n}}$ is

the wave vector of the scattered SFG field, $\mathbf{k}_{SF}^{0} = \mathbf{k}_{IR} + \mathbf{k}_{VIS}$ and $\mathbf{q}$ is the scattering wave vector, defined as $\mathbf{k}_{SF} - \mathbf{k}_{SF}^{0} = q\hat{\mathbf{q}} = 2k_{SF}\sin\frac{\theta}{2}\hat{\mathbf{q}}$.

For the case of HHH polarization the transverse scattered field from a single sphere can be calculated from Eq. (2) to be

$$E_{SF}(r) = -E_{IR}E_{VIS}k_{SF}^{2}\frac{e^{ik_{SF}r}}{2\epsilon r}\Big\{\cos\frac{\theta}{2}[(\Gamma^{(2)}_{\perp\perp\perp} + \Gamma^{(2)}_{\perp\parallel\parallel})\cos\beta + (\Gamma^{(2)}_{\perp\perp\perp} - \Gamma^{(2)}_{\perp\parallel\parallel})\cos(\theta - \beta + 2\alpha)] - \sin\frac{\theta}{2}[(\Gamma^{(2)}_{\parallel\parallel\perp} - \Gamma^{(2)}_{\parallel\perp\parallel})\sin\beta + (\Gamma^{(2)}_{\parallel\perp\parallel} + \Gamma^{(2)}_{\parallel\parallel\perp})\sin(\theta - \beta + 2\alpha)]\Big\}, \quad (3)$$

where $\Gamma^{(2)}_{iii}$ is a function of the local second-order susceptibility elements and the experimental observables R and θ as defined in Table I. It is insightful to express the nonlinearly scattered sum frequency field in terms of an effective nonlinear susceptibility of a single sphere, $\mathbf{\Gamma}^{(2)}$, because it allows us to describe the nonlinear surface scattering from one sphere at a particular angle in a way similar to conventional sum frequency generation from a planar surface [26]. Corresponding expressions for the other polarization combinations can also be derived. Of the eight possible polarization combinations only four generate nonzero expressions: HHH, VVH, VHV, and HVV (shown in Fig. 2). This can be understood from simple symmetry arguments [27]: Reflection ($y \rightarrow -y$) in the horizontal x-z plane changes the sign of vertically (V) polarized fields but does not affect horizontally (H) polarized waves. Since the system is symmetric under this reflection, only those combinations which involve an even number of vertically polarized fields are symmetry allowed. Equation (3) reduces to the results reported earlier [13,14] for second harmonic scattering if $\boldsymbol{\chi}^{(2)}$ is dominated by the radial component (i.e., $\boldsymbol{\chi}^{(2)} = 0$, except for $\chi^{(2)}_{\perp\perp\perp}$).

From Eq. (3) it is clear that for a given scattering angle the transverse component of $\mathbf{E}_{SF}$ is a linear combination of the components of the effective nonlinear spherical susceptibility $\mathbf{\Gamma}^{(2)}$. This is equivalent to the description of VSFG from a planar interface [28]. Hence, we can still model the spectra using the familiar expressions for VSFG [3,6,12]:

$$\mathbf{E}_{SF} \propto \sum_{n}\mathbf{\Gamma}^{(2)}_{n}:\mathbf{E}_{IR}\mathbf{E}_{VIS} \qquad \Gamma^{(2)}_{n}(\omega) = \frac{A_n}{(\omega - \omega_{0n}) + i\Upsilon_n}, \quad (4)$$

TABLE I. Values of the elements of the effective second-order susceptibility $\mathbf{\Gamma}^{(2)}$ in terms of the local susceptibilities $\boldsymbol{\chi}^{(2)}$ and experimental observables, θ and R.

$\Gamma^{(2)}_{\perp\perp\perp}$	$2\pi[B\chi^{(2)}_{\perp\perp\perp} + A(\chi^{(2)}_{\perp\parallel\parallel} + \chi^{(2)}_{\parallel\perp\parallel} + \chi^{(2)}_{\parallel\parallel\perp})]$
$\Gamma^{(2)}_{\perp\parallel\parallel}$	$\pi[A\chi^{(2)}_{\perp\perp\perp} + (A + 2B)\chi^{(2)}_{\perp\parallel\parallel} - A(\chi^{(2)}_{\parallel\perp\parallel} + \chi^{(2)}_{\parallel\parallel\perp})]$
$\Gamma^{(2)}_{\parallel\perp\parallel}$	$\pi[A(\chi^{(2)}_{\perp\perp\perp} - \chi^{(2)}_{\perp\parallel\parallel}) + (A + 2B)\chi^{(2)}_{\parallel\perp\parallel} - A\chi^{(2)}_{\parallel\parallel\perp}]$
$\Gamma^{(2)}_{\parallel\parallel\perp}$	$\pi[A(\chi^{(2)}_{\perp\perp\perp} - \chi^{(2)}_{\perp\parallel\parallel}) - A\chi^{(2)}_{\parallel\perp\parallel} + (A + 2B)\chi^{(2)}_{\parallel\parallel\perp}]$
A	$\frac{6i}{q^4R^2}\{2(1 - \frac{q^2R^2}{3})\sin(qR) - 2qR\cos(qR)\}$
B	$\frac{6i}{q^4R^2}\{(q^2R^2 - 2)\sin(qR) - qR(\frac{q^2R^3}{3} - 2)\cos(qR)\}$

where n refers to a vibrational mode, ω_{0n} is the resonance frequency, and Υ_n is the spectral half width at half maximum. The solid lines in Fig. 2 are fits of the data to the convolution $I_{SF}(\omega_{VIS} + \omega_{IR}) \propto |\sum_n \Gamma^{(2)}_n(\omega_{IR}) \otimes E_{VIS}(\omega_{VIS})|^2$ of Eq. (4) and the derived electric field envelope of the up-conversion pulse E_{VIS}. The fits were obtained using all five well-known CH stretch resonances [10]: the symmetric CH_3 and CH_2 stretches at 2890 and 2853 cm^{-1}, the asymmetric CH_3 and CH_2 stretches at 2980 and 2910 cm^{-1}, and a Fermi resonance at 2930 cm^{-1}. The central frequencies were obtained from a linear infrared spectrum and a Raman spectrum of the same colloid sample. For planar surfaces it is well established that alkane chains in an ordered all-trans conformation possess inversion symmetry around the CH_2 groups, which, as a consequence, do not appear in the sum frequency spectrum [4,5,7,12]. As the CH_2 group distances are very small compared to the particle dimensions, this selection rule still applies and thus we can conclude from the relatively strong contribution from the CH_2 groups to the spectrum that the stearyl chains are not well ordered on the surface. If we compare this to a structure of a Langmuir film the structure must be an open one with many gauche defects in the alkane chains, much like the uncompressed liquid expanded phase of a phospholipid monolayer [12].

Figure 3 shows a radial distribution pattern of the square of the amplitude ($|A_{sym.CH_3}|^2$) of the CH_3 symmetrical stretch mode, obtained from fits to spectra measured at different angles. Similar to previous theoretical [15] and experimental [13] results for SHG scattering, the sum frequency signal vanishes in the forward direction (i.e., at $\theta = 0$) in agreement with Eq. (2). This effect is a direct consequence of the inversion symmetry of the particles. At $\theta \neq 0$ the variation of the phase mismatch across the sphere effectively lifts the inversion symmetry, leading to a finite scattering intensity. The solid line represents the calculated emitted power ($\frac{dP}{d\Omega} = \frac{cr^2\sqrt{\epsilon}}{2\pi}|E|^2$) over a solid angle of 12°. The fit results in amplitudes of the local surface susceptibility for this mode of $\chi^{(2)}_{\perp\parallel\parallel}/\chi^{(2)}_{\perp\perp\perp} = -0.29$, $\chi^{(2)}_{\parallel\perp\parallel}/\chi^{(2)}_{\perp\perp\perp} = 0.28$, and $\chi^{(2)}_{\parallel\parallel\perp}/\chi^{(2)}_{\perp\perp\perp} = 0.32$. With these parameters the intensity ratio of the different polarization combinations as presented in Fig. 2 can be reproduced very well. This shows that for this submicron sized particle type of system the RGD approach is well suited to describe the experimental

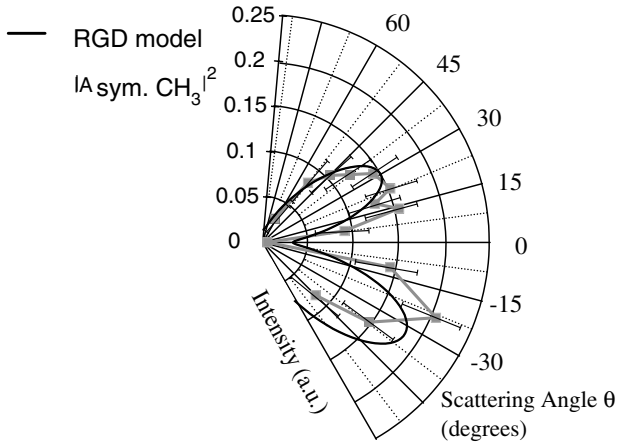

FIG. 3. Polar plot of the angular distribution of SFG intensity for the symmetrical CH_3 stretch mode. The solid line is a fit through the data using Eq. (3). $\theta = 0$ is defined as the phase matching angle.

results and allows for an accurate estimate of the relative magnitudes of the different elements of the local nonlinear susceptibility.

To summarize, we have measured vibrational sum frequency spectra for a dispersion of submicron sized particles covered with alkane chains. By analyzing the results using a Rayleigh-Gans-Debye approximation we obtain information about the local molecular order and density of these chains on the surface of the particle. This extension of SFG to nonplanar surfaces demonstrates that this technique with its inherent molecular surface sensitivity can now be applied to a wider range of systems. This opens new avenues for the *in situ* research of the surfaces of, e.g., cells, vesicles, particles, and related systems.

The authors thank M. Pronk, R. C. V. van Schie, and P. Schakel for excellent technical support, T. F. Heinz, H. N. W. Lekkerkerker, C. M. van Kats, and A. van Blaaderen for many helpful discussions, and J. den Dulk for making equipment available to us. This work is part of the research program of the Foundation for Fundamental Research on Matter (FOM) and is supported by the Netherlands Organization for Scientific Research (NWO).

*Electronic address: roke@chem.leidenuniv.nl

[1] G. A. Reider and T. F. Heinz, in *Photonic Probes of Surfaces* (Elsevier, Amsterdam, 1995), Chap. 9.
[2] Y. R. Shen, Nature (London) **337**, 519 (1989).
[3] T. F. Heinz, in *Nonlinear Surface Electromagnetic Phenomena*, edited by H. E. Ponath and G. I. Stegeman (Elsevier, New York, 1991), Chap. 5.
[4] R. A. Walker, J. A. Gruetzmacher, and G. L. Richmond, J. Am. Chem. Soc. **120**, 6991 (1998).
[5] T. Petralli-Mallow, K. Briggman, L. Richter, J. Stephenson, and A. Plant, Proc. SPIE-Int. Soc. Opt. Eng. **3858**, 25 (1999).
[6] J. H. Hunt, P. Guyot-Sionnest, and Y. R. Shen, Chem. Phys. Lett. **133**, 189 (1987).
[7] P. Guyot-Sionnest, J. H. Hunt, and Y. R. Shen, Phys. Rev. Lett. **59**, 1597 (1989).
[8] P. B. Miranda, V. Pflumnio, H. Saijo, and Y. R. Shen, J. Am. Chem. Soc. **120**, 12 092 (1998).
[9] E. C. Y. Yan and K. B. Eisenthal, J. Phys. Chem. B **103**, 6056 (1999).
[10] X. Zhuang, P. B. Miranda, D. Kim, and Y. R. Shen, Phys. Rev. B **59**, 12 632 (1999).
[11] D. Zhang, J. Gutow, and K. B. Eisenthal, J. Phys. Chem. **98**, 13 729 (1994).
[12] S. Roke, J. Schins, M. Müller, and M. Bonn, Phys. Rev. Lett. **90**, 128101 (2003).
[13] N. Yang, W. E. Angerer, and A. G. Yodh, Phys. Rev. Lett. **87**, 103902 (2001).
[14] J. Martorell, R. Vilaseca, and R. Corbalán, Phys. Rev. A **55**, 4520 (1997).
[15] J. I. Dadap, J. Shan, K. B. Eisenthal, and T. F. Heinz, Phys. Rev. Lett. **83**, 4045 (1999).
[16] G. Ma and H. C. Allen, J. Am. Chem. Soc. **124**, 9374 (2001).
[17] T. Kawai, D. J. Neivandt, and P. B. Davies, J. Am. Chem. Soc. **122**, 12 031 (2000).
[18] T. S. Koffas, J. Kim, C. C. Lawrence, and G. A. Somorjai, Langmuir **19**, 3563 (2003).
[19] E. W. M. van der Ham, Q. H. F. Vrehen, and E. R. Eliel, Surf. Sci. **368**, 96 (1996).
[20] L. J. Richter, T. P. Petralli-Mallow, and J. C. Stephenson, Opt. Lett. **23**, 1594 (1998).
[21] A. van Helden, J. Jansen, and A. Vrij, J. Colloid Interface Sci. **81**, 354 (1981).
[22] W. Stöber, A. Vink, and R. Bohn, J. Colloid Interface Sci. **26**, 62 (1968).
[23] H. C. van de Hulst, *Light Scattering by Small Particles* (John Wiley & Sons, New York, 1957).
[24] W. Brown, *Light Scattering, Principles and Development* (Clarendon Press, Oxford, 1996).
[25] D. E. Gray, *American Institute of Physics Handbook* (McGraw-Hill, New York, 1982).
[26] S. Roke, M. Bonn, and A. V. Petukhov (to be published).
[27] R. W. Boyd, *Nonlinear Optics* (Academic Press, New York, 1992).
[28] Y. R. Shen, *The Principles of Nonlinear Optics* (Wiley, New York, 1984).